[8]Middleton, R. H., *Delta Toolbox for Use with MATLAB*™, The Mathworks, Natick, MA, 1990.
[9]O'Brien, M. J., and Broussard, J. R., "Feedforward Control to Track the Output of a Forced Model," *Proceedings of the 17th IEEE Conference on Decision and Control* (San Diego, CA), Inst. for Electrical and Electronics Engineers, Piscataway, NJ, 1978, pp. 1149–1155.
[10]Grace, A., *Optimization Toolbox for Use with MATLAB*™, *User's Guide*, The Mathworks, Natick, MA, 1990.

Relation between Modified Sparse Time Domain and Eigensystem Realization Algorithm

An-Pan Cherng* and Mohamed K. Abdelhamid†
University of Maryland at College Park, College Park, Maryland 20742

Introduction

A WIDELY used time-domain modal parameter estimation approach is to seek a candidate characteristic polynomial whose roots correspond to natural frequencies and damping ratios. For suboptimal solutions the polynomial may be calculated by least squares (LS) or total least squares (TLS) fitting techniques, where the latter estimates correct modal parameters statistically. The LS solutions include the Ibrahim time domain (ITD),[1] sparse time domain (STD),[2] polyreference method,[3] and eigensystem realization algorithm (ERA).[4] The TLS solution mainly utilizes a subspace orthogonality concept to separate signal and noise subspaces and then extracts signal information (including natural frequency and damping) from either subspace. In other words TLS seeks an unbiased characteristic polynomial whose roots correspond to structural modes. Polynomial root finding (or equivalently the eigenvalue problem of a companion matrix) is time consuming for a highly overspecified polynomial when noise is present in the measured data. In a realization type of solution, such as ERA, model reduction is first performed to eliminate the extraneous, computational modes and a reduced eigenvalue problem is then solved. A recently proposed modified sparse time-domain (MSTD) method (Tasker and Chopra[5]) combines the accuracy in TLS and the speed in the reduced eigenvalue problem. It has been reported to be superior to STD in both accuracy and speed. In this Note we will provide an alternative way to derive the same MSTD formulation (the second and noniterative method of Tasker and Chopra) and indicate multi-input, multi-output (MIMO) applicability. We will show by reason and example that in fact the performance of MSTD is very close to the ERA but with less bias.

New Derivation of MSTD

Consider a linear, viscously damped structure that is tested in a single-input, single-output (SISO) format. The Hankel matrix $\boldsymbol{H}$ composed of sampled impulse responses, y_k, $k = 0, 1, 2, \ldots$, is

$$\boldsymbol{H} = \begin{bmatrix} y_1 & y_2 & \cdots & \cdots & y_m \\ y_2 & y_3 & \cdots & \cdots & y_{m+1} \\ \cdots & \cdots & \cdots & \cdots & \cdots \\ y_{r-1} & y_r & \cdots & \cdots & y_{m+r-2} \\ y_r & y_{r+1} & \cdots & \cdots & y_{m+r-1} \end{bmatrix}$$

$$y_k = \sum_{i=1}^{n} A_i \exp(\lambda_i k \Delta t) + \sum_{i=1}^{n} A_i^* \exp(\lambda_i^* k \Delta t)$$

where y_k contains $2n$ complex conjugate modes and λ_i contains the ith natural frequency and damping ratio.

Suppose we partition $\boldsymbol{H}$ into a submatrix and a vector in two ways:

$$\boldsymbol{H} = [\boldsymbol{H}_1 \quad \boldsymbol{h}_1] = [\boldsymbol{h}_2 \quad \boldsymbol{H}_2] \tag{1}$$

where $\boldsymbol{h}_1$ and $\boldsymbol{h}_2$ are the last and first column vectors of $\boldsymbol{H}$ and $\boldsymbol{H}_1$ and $\boldsymbol{H}_2$ are their complementary submatrices. Here $\boldsymbol{H}_2$ and $\boldsymbol{H}_1$ are related by

$$\boldsymbol{H}_2 = \boldsymbol{H}_1 \boldsymbol{B} \quad \text{or} \quad \boldsymbol{B} = \boldsymbol{H}_1^+ \boldsymbol{H}_2 \tag{2}$$

where the plus superscript denotes a pseudoinverse. Matrix $\boldsymbol{B}$ has observability companion form and is upper Hessenberg. Part of the eigenvalues of the coefficient matrix $\boldsymbol{B}$ correspond to structural modes and others correspond to noise modes.

Taking the SVD of a noisy and overspecified $\boldsymbol{H}_1$ yields

$$\boldsymbol{H}_1 = \boldsymbol{P}_{1s} \Sigma_{1s} \boldsymbol{Q}_{1s}^T + \boldsymbol{P}_{1n} \Sigma_{1n} \boldsymbol{Q}_{1n}^T = \boldsymbol{H}_{1s} + \boldsymbol{H}_{1n} \tag{3}$$

where Σ_{1s} contains larger singular values, $\boldsymbol{H}_{1s}$ stands for the signal matrix, matrices $\boldsymbol{P}$ and $\boldsymbol{Q}$ are orthogonal, and $\boldsymbol{P}_{1s}$ and $\boldsymbol{Q}_{1s}$ span the exact left and right noiseless signal subspaces. The reduced solution is

$$\boldsymbol{B} = \boldsymbol{H}_{1s}^+ \boldsymbol{H}_2 = \boldsymbol{Q}_{1s} \Sigma_{1s}^{-1} \boldsymbol{P}_{1s}^T \boldsymbol{H}_2 \tag{4}$$

We further decompose $\boldsymbol{H}_{1s}$ into a product of two matrices, i.e.,

$$\boldsymbol{H}_{1s} = \boldsymbol{P}_{1s} \Sigma_{1s} \boldsymbol{Q}_{1s}^T = \boldsymbol{S}_{1s} \boldsymbol{S}_{2s}^T \tag{5}$$

A smaller coefficient matrix $\bar{\boldsymbol{B}}$ can be calculated by

$$\bar{\boldsymbol{B}} = \boldsymbol{S}_{2s}^T \boldsymbol{B} (\boldsymbol{S}_{2s}^T)^+ = \boldsymbol{S}_{1s}^+ \boldsymbol{H}_2 (\boldsymbol{S}_{2s}^T)^+ \tag{6}$$

Matrices $\boldsymbol{B}$ and $\bar{\boldsymbol{B}}$ are similar, or pseudosimilar, in the sense that all eigenvalues of the smaller matrix $\bar{\boldsymbol{B}}$ belong to those of $\boldsymbol{B}$. The ERA uses a balanced decomposition for $\boldsymbol{S}_{1s}$ and $\boldsymbol{S}_{2s}$ where

$$\boldsymbol{S}_{1s} = \boldsymbol{P}_{1s} \Sigma_{1s}^{1/2} \qquad \text{and} \qquad \boldsymbol{S}_{2s}^T = \Sigma_{1s}^{1/2} \boldsymbol{Q}_{1s}^T \tag{7}$$

If the reduced size of $\bar{\boldsymbol{B}}$ is equal to the number of active complex conjugate modes ($= 2n$), extraneous (i.e., noise) modes will be excluded.

To demonstrate the relation between MSTD and the ERA, let

$$\boldsymbol{H}_s = \boldsymbol{S}_1 \boldsymbol{S}_2^T = \boldsymbol{P}_1 \Sigma_1 \boldsymbol{Q}_1^T \tag{8}$$

The TLS solution of the polynomial vector orthogonal to $\boldsymbol{H}_s$ is

$$\boldsymbol{Q}_1^T \bar{\boldsymbol{b}} = \boldsymbol{0} \qquad \text{or} \qquad \boldsymbol{S}_2^T \bar{\boldsymbol{b}} = \boldsymbol{0} \tag{9}$$

Now suppose $\boldsymbol{S}_2$ can be partitioned in two ways:

$$\boldsymbol{S}_2 = \begin{bmatrix} \boldsymbol{G}_1 \\ \boldsymbol{g}_1^T \end{bmatrix} = \begin{bmatrix} \boldsymbol{g}_2^T \\ \boldsymbol{G}_2 \end{bmatrix} \tag{10}$$

where $\boldsymbol{g}_1^T$ and $\boldsymbol{g}_2^T$ are the last and first row vectors and $\boldsymbol{G}_1$ and $\boldsymbol{G}_2$ are their complementary submatrices, respectively. The monic characteristic polynomial vector and $\boldsymbol{S}_2$ are orthogonal to each other, i.e.,

$$\boldsymbol{S}_2^T \bar{\boldsymbol{b}} = [\boldsymbol{G}_1^T \quad \boldsymbol{g}_1] \begin{bmatrix} \boldsymbol{b} \\ 1 \end{bmatrix} = 0 \tag{11}$$

The leading coefficient, 1, may be replaced by an identity matrix if multiple inputs are used.[6] Since $\boldsymbol{S}_2$ represents the right signal subspace of $\boldsymbol{H}$, its submatrix $\boldsymbol{G}_1$ also approximates the right signal subspace of $\boldsymbol{H}_1$ (with one row shorter). Using Eq. (6), we get

$$\bar{\boldsymbol{B}} = \boldsymbol{G}_1^T \boldsymbol{B} (\boldsymbol{G}_1^T)^+ = \boldsymbol{G}_1^T \left[\begin{array}{c|c} \boldsymbol{0} & -\boldsymbol{b} \\ \boldsymbol{I} & \end{array} \right] (\boldsymbol{G}_1^T)^+ \tag{12}$$

Received May 21, 1993; revision received August 26, 1993; accepted for publication Sept. 28, 1993.

*Currently Associate Professor, National I-Lan Institute of Agriculture and Technology.
†Currently Staff Scientist, AlliedSignal Automotive, 401 N. Bendix Drive, South Bend, IN 46634.

and using the relations

$$\bar{\boldsymbol{B}} = \boldsymbol{G}_2^T(\boldsymbol{G}_1^T)^+ \tag{13}$$

$$\boldsymbol{G}_1^T = \boldsymbol{G}_1(\boldsymbol{G}_1^T\boldsymbol{G}_1)^{-1} \tag{14}$$

$$\boldsymbol{S}_2^T\boldsymbol{S}_2 = [\boldsymbol{G}_1^T \quad \boldsymbol{g}_1]\begin{bmatrix}\boldsymbol{G}_1\\ \boldsymbol{g}_1^T\end{bmatrix} = \boldsymbol{G}_1^T\boldsymbol{G}_1 + \boldsymbol{g}_1\boldsymbol{g}_1^T = \boldsymbol{I} \tag{15}$$

$$\boldsymbol{G}_1^T\boldsymbol{G}_1 = \boldsymbol{I} - \boldsymbol{g}_1\boldsymbol{g}_1^T \tag{16}$$

$$(\boldsymbol{G}_1^T\boldsymbol{G}_1)^{-1} = \left\{\boldsymbol{I} + \boldsymbol{g}_1(\boldsymbol{I} - \boldsymbol{g}_1^T\boldsymbol{g}_1)^{-1}\boldsymbol{g}_1^T\right\} \tag{17}$$

$\bar{\boldsymbol{B}}$ is finally expressed as

$$\bar{\boldsymbol{B}} = \boldsymbol{G}_2^T\boldsymbol{G}_1\left\{\boldsymbol{I} + \boldsymbol{g}_1(\boldsymbol{I} - \boldsymbol{g}_1^T\boldsymbol{g}_1)^{-1}\boldsymbol{g}_1^T\right\} \tag{18}$$

which is identical to the MSTD (the second method of Tasker).

For the MIMO case, the original signal subspace is partitioned into a block submatrix and a block vector in which each element has size $(q \times q)$ if q inputs are used.

To compare with the ERA, we notice that SVD is performed on $\boldsymbol{H}_1$ for the ERA and on $\boldsymbol{H}$ (one column larger than $\boldsymbol{H}_1$) for MSTD. Comparing Eq. (6) of the ERA with Eq. (12) of MSTD, we find that the major difference between the ERA and MSTD is the polynomial vector in the companion matrix. The ERA uses the biased polynomial, which can be estimated by SVD, whereas MSTD uses the unbiased polynomial from TLS. In other words, their difference is mainly in how the polynomial vector is obtained using LS or TLS. As a result, it would be thought that MSTD has less bias than the ERA (or the LS matrix approach). In addition, when the number of data points used approaches infinity, the noise contained in the estimated signal subspace also vanishes (provided that the uncorrelation assumption of signal and noise is satisfied). Thus, MSTD is asymptotically unbiased, whereas the ERA is still asymptotically biased (from the biased polynomial). But their close resemblance is still clear.

In practice, only finite data points are available. The estimate of signal subspace is thus unlikely to be without noise component (even though it is unbiased statistically). When there is any noise present in the estimated signal subspace, the inversion of $\boldsymbol{G}_1^T$ in Eq. (13) indicates that MSTD will result in biased estimates unless the iterations of estimating the signal subspace are as suggested in the first method of Tasker and Chopra.[5] In other words, the unbiased property of MSTD will be obtained only when the signal subspace is perfectly estimated (not just unbiasedly estimated). This raises a question of whether the unbiased polynomial vector used in MSTD dramatically reduces the bias in the solution compared to the ERA. An intuitive thought would be that, since the difference between $\boldsymbol{H}$ and $\boldsymbol{H}_1$ is only one column, the difference will become insignificant as the size of the Hankel matrices increases. Therefore, close performance of MSTD and the ERA should be expected. However, we may still state that under moderate signal-to-noise ratio (SNR) and finite data points, the performance of MSTD is expected to be more accurate than that of ERA due to the unbiased polynomial used.

Illustrative Example

To compare MSTD with the ERA, consider the SISO impulse response

$$y_k = \sum_{i=1}^{2} A_i \exp(-\lambda_i\zeta_i k\Delta t)\sin\left(\sqrt{1-\zeta_i^2}\lambda_i k\Delta t\right)$$

$$k = 0, 1, 2, \ldots$$

with

$$A_1 = 1.0 \qquad \lambda_1 = 1.0\ \text{Hz} \qquad \zeta_1 = 0.02$$
$$A_2 = 1.2 \qquad \lambda_2 = 1.2\ \text{Hz} \qquad \zeta_2 = 0.02$$
$$\Delta t = 0.2$$

A maximum of 200 sampled data are used to construct the Hankel matrix.

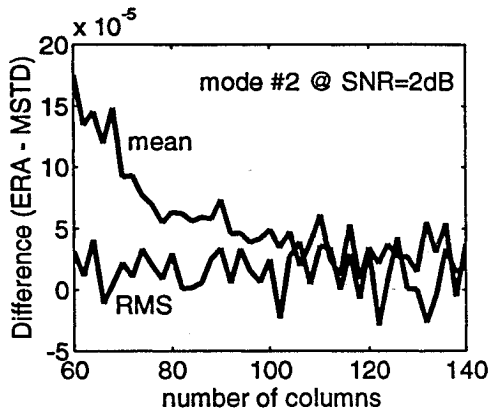

Fig. 1 Difference between ERA and MSTD.

Let the variance of a random noise be σ^2 and the total number of points used be N. The SNR is defined by

$$\text{SNR (dB)} = 10\log_{10}\left(\frac{1}{N\sigma^2}\sum_{k=1}^{N} y_k^2\right)$$

The mean value and averaged root-mean-square (RMS) error of each mode are presented for comparison. The averaged RMS error for mode i is defined by

$$\text{RMS}_i = \sqrt{\frac{1}{100}\sum_{k=1}^{100}(\hat{\zeta}_i(k) - \zeta_i)^2} \qquad i = 1, 2$$

The number of columns c_n is increased from 60 to 140 with an increment of 2 columns at each step. The results are depicted in Fig. 1.

We can see that in most cases MSTD does have better performance over the ERA, as we expected. In Fig. 1, the difference in mean value drops as c_n increases (but still above the zero line). The difference of the RMS error in Fig. 1 also shows that MSTD is slightly better than the ERA. The difference in the RMS error indicates that for c_n less than the center ($c_n = 100$) MSTD always performs better than the ERA; but it gradually loses this superiority as c_n increases. The above observations suggest that the noise component in the estimated signal subspace degrades the performance of both methods.

The results at 5 dB SNR (not shown) indicate that the difference between MSTD and the ERA grows as the noise level increases and that a larger difference is observed at lower c_n for each curve. This indicates that the bias of the polynomial vector in the ERA degrades the results.

Conclusions

An alternative derivation of MSTD has been provided in this Note along with possibility for extension to the MIMO case. It has been shown that the use of shifted signal subspace components in MSTD is a hybrid solution, which combines the accuracy in TLS and the model reduction in the ERA.

For a finite number of data points, the performance of MSTD is very close to the ERA but with more accuracy, as evidenced by the example given in this paper. Thus the result of MSTD is as reliable as the ERA. It should be noted, however, the MSTD utilizes the companion structure and the data in the Hankel matrix must be sequentially filled.

Acknowledgments

This research was performed under a State of Maryland MIPS project, sponsored by Manufacturing and Technology Conversion International, Inc., Columbia, MD. The authors would also like to thank F. Tasker for many valuable discussions.

References

[1]Ibrahim, S. R., and Mikulcik, E. C., "A Method for the Direct Identification of Vibration Parameters from Free Response," *Shock and Vibration Bulletin*, No. 47, 1977, pp. 183–198.

[2]Ibrahim, S. R., "An Upper Hessenberg Sparse Matrix Algorithm for Modal Identification on Minicomputers," *Journal of Sound and Vibration*, Vol. 113, No. 1, 1987, pp. 47–55.

[3]Vold, H., Kundrat, J., Rocklin, G. T., and Russell, R., "A Multi-input Modal Estimation Algorithm for Minicomputers," SAE Paper 820194, 1982.

[4]Juang, J. N., and Pappa, R. S., "An Eigensystem Realization Algorithm for Modal Parameter Identification and Model Reduction," *Journal of Guidance, Control, and Dynamics*, Vol. 8, No. 5, 1985, pp. 620–627.

[5]Tasker, F., and Chopra, I., "Modified Sparse Time Domain Technique for Rotor Stability Testing," *Journal of Guidance, Control, and Dynamics*, Vol. 15, No. 6, 1992, pp. 1366–1374.

[6]Cherng, A. P., "Identification of Pseudo Stationary Modal Parameters—Updating and Detection," Ph.D. Dissertation, Department of Mechanical Engineering, Univ. of Maryland—UMBC, Jan. 1993.

Modeling and Simulation of Rotor Bearing Friction

Arun K. Banerjee*
Lockheed Palo Alto Research Laboratory, Palo Alto, California 94304
and
Thomas R. Kane†
Stanford University, Stanford, California 94305

Introduction

MODELING of friction is an important subject in all situations involving contacting surfaces, and various friction models exist in the literature.[1–4] Reference 2 evaluated several such models and came to the conclusion that all models except the classical Coulomb model simulated equally well motion under friction observed experimentally. This paper revisits four ways of modeling friction in bearings and examines these in the context of simulation of motion of a simple system, namely, a compound pendulum (a payload) supported by a journal bearing. The friction models considered are Coulomb friction, Dahl friction, and two friction models not considered in Ref. 2, namely, the friction circle model[5] and viscous friction. It is shown that a realistic treatment of Coulomb friction[6] in a rotor bearing requires the consideration of a two-degree-of-freedom model and the formulation of three sets of dynamical equations, one valid for slipping, one for sticking, and a third for transition from sticking to slipping. The other three friction models do not require such complex modeling and give rise to simpler simulations. The price of such simplicity, as numerical results show, however, is that, even though the motion of the pendulum predicted by all friction models is essentially the same, none of the models except the Coulomb model provides the detailed information on high-frequency chatter and the stick-slip nature of the motion.

Journal Bearing Friction: An Example

A pendulum with friction at its hinge provides a simple system involving rotor bearing friction. Figure 1 shows a compound pendulum B mounted in a bearing, with points O and O' being, respectively, the centers of the bearing and the journal, the bearing clearance having been exaggerated for the sake of clarity. The pendulum is of mass m and centroidal inertia J, the journal radius is r and the bearing radius R; and the distance from O' to B^*, the mass center of B, is L along the unit vector $\bar{b}_1$.

Received Oct. 6, 1993; revision received Dec. 21, 1993; accepted for publication Jan. 3, 1994.

*Senior Staff Engineer. Associate Fellow AIAA.
†Emeritus Professor, Division of Applied Mechanics.

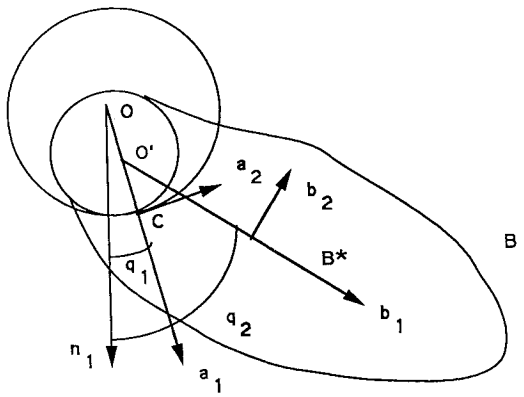

Fig. 1 Compound pendulum mounted in rotor bearing.

Coulomb Friction Model

A fundamental fact that has not received sufficient attention in the literature on bearing dynamics is that simple rotation of a rigid body attached to a journal rotating in a bearing gives rise to a two-degree-of-freedom problem. This is illustrated in Fig. 1, where the journal, which is a part of B, contacts the bearing at point C. The angles q_1 and q_2 that the lines OC and $O'B^*$ make, respectively, with a line fixed in the inertial frame characterize the two degrees of freedom of B. Coulomb's law of friction states that friction at the contact point C prevents the bodies from sliding so long as the tangential force at C does not exceed $\mu_s N$, where μ_s is the static coefficient of friction and N is the normal force; once sliding occurs, the friction force $\bar{\tau}$ is described by

$$\bar{\tau} = -\mu_k N \frac{\bar{v}^C}{|\bar{v}^C|} \tag{1}$$

where μ_k is the kinetic coefficient of friction and $\bar{v}^C$ is the velocity of the point C of B that is in contact with the bearing. The equations of motion of the pendulum during sliding are

$$m[(R-r)\ddot{q}_1 + L\ddot{q}_2\cos(q_2-q_1) - L\dot{q}_2^2\sin(q_2-q_1) + g\sin q_1] = -\mu_k N \operatorname{sign}[(R-r)\dot{q}_1 + r\dot{q}_2] \tag{2}$$

$$mL[(R-r)\ddot{q}_1\cos(q_2-q_1) + L\ddot{q}_2 + (R-r)\dot{q}_1^2\sin(q_2-q_1) + gL\sin q_2] + J\ddot{q}_2 = -\mu_k rN \operatorname{sign}[(R-r)\dot{q}_1 + r\dot{q}_2] \tag{3}$$

where N, the normal reaction at the contact point, is given by

$$N = m[(R-r)\dot{q}_1^2 + L\ddot{q}_2\sin(q_2-q_1) + L\dot{q}_2^2\cos(q_2-q_1) + g\cos q_1] \tag{4}$$

Sliding gives way to rolling when the velocity of the contact point is equal to zero, in which event

$$(R-r)\dot{q}_1 + r\dot{q}_2 = 0 \tag{5}$$

In numerical simulations, the zero on the right-hand side of Eq. (5) is replaced by ϵ_1, a small number chosen arbitrarily. With rolling, the number of degrees of freedom of the system is reduced to 1, and the equation of motion becomes

$$\{m[r^2 - 2rL\cos(q_2-q_1) + L^2] + J\}\ddot{q}_2 = -\frac{R}{R-r}mrL\dot{q}_2^2\sin(q_2-q_1) + mg(r\sin q_1 - L\sin q_2) \tag{6}$$

This equation is valid so long as the tangential force at the contact point is smaller than the static friction force. For the pendulum supported by the bearing, this condition is expressed as

$$|m(\bar{a}^{B^*} - g\bar{n}_1)\cdot\bar{a}_2| \le \mu_s N \tag{7}$$

where $\bar{a}^{B^*}$ is the acceleration of B^*, g is the acceleration due to gravity, $\bar{a}_2$ is a unit vector parallel to the tangent to the contact